TLR4 signaling augments B lymphocyte migration and overcomes the restriction that limits access to germinal center dark zones

Il-Young Hwang, Chung Park, Kathleen Harrison, and John H. Kehrl

Laboratory of Immunoregulation, National Institute of Allergy and Infectious Diseases, National Institutes of Health, Bethesda, MD 20892

B lymphocyte–intrinsic Toll-like receptor (TLR) signals amplify humoral immunity and can exacerbate autoimmune diseases. We identify a new mechanism by which TLR signals may contribute to autoimmunity and chronic inflammation. We show that TLR4 signaling enhances B lymphocyte trafficking into lymph nodes (LNs), induces B lymphocyte clustering and interactions within LN follicles, leads to sustained in vivo B cell proliferation, overcomes the restriction that limits the access of nonantigen-activated B cells to germinal center dark zones, and enhances the generation of memory and plasma cells. Intravital microscopy and in vivo tracking studies of B cells transferred to recipient mice revealed that TLR4-activated, but not nonstimulated, B cells accumulated within the dark zones of preexisting germinal centers even when transferred with antigen-specific B cells. The TLR4-activated cells persist much better than nonstimulated cells, expanding both within the memory and plasma cell compartments. TLR-mediated activation of B cells may help to feed and stabilize the spontaneous and ectopic germinal centers that are so commonly found in autoimmune individuals and that accompany chronic inflammation.

CORRESPONDENCE
John H. Kehrl:
jkehrl@niaid.nih.gov

Abbreviations used: BAFF, B cell–activating factor of the tumor necrosis factor family; BCR, B cell antigen receptor; FDC, follicular DC; HEL, hen egg lysozyme; iLN, inguinal LN; MIP, maximum intensity projection; PLN, popliteal LN; TLR, toll-like receptor; TP-LSM, two-photon laser-scanning microscopy; TRIF, TIR domain–containing adapter-inducing IFN-β .

Toll-like receptors (TLRs) were first identified as receptors for microbial products that trigger innate immunity (Beutler and Rietschel, 2003). All TLR receptors, with the exception of TLR3, use the adaptor protein MyD88 and are capable of activating NF-κB. TLR3 and TLR4 receptors couple to the TIR domain–containing adapter-inducing IFN-β (TRIF), which triggers type I IFN production. Naive mouse B cells express a variety of TLRs and can be polyclonally stimulated by either TLR4 or TLR9 ligands to proliferate and differentiate into Ig-secreting cells. The role of TLRs in T cell–dependent immune responses in mice is controversial, as one study has shown a requirement for TLR activation, whereas others have shown that TLR signals only help to amplify the responses (Pasare and Medzhitov, 2005; Gavin et al., 2006; Meyer-Bahlburg et al., 2007). The TLR repertoire of human B cells differs somewhat from that of mice, as naive human B cells have low levels of TLR expression. However, B cell antigen receptor (BCR) stimulation induces strong expression of TLR6, TLR7, TLR9, and TLR10 (Peng, 2005). The proliferation and differentiation of naive human B cells to Ig-secreting cells may require exposure to TLR ligands in addition to a BCR signal and a cognate interaction with helper T cells (Ruprecht and Lanzavecchia, 2006). Like naive mouse B cells, human memory B cells constitutively express several TLRs, although not TLR4, and can respond directly to TLR stimulation (Bernasconi et al., 2003). The treatment of human peripheral blood B cells with TLR7 or TLR9 agonists induces increased cytokine and chemokine production as well as the secretion of IgG and IgM (Hanten et al., 2008).

Inappropriate TLR signaling has been associated with autoimmunity (Krieg and Vollmer, 2007). TLR4 up-regulation can break immunological tolerance and induce a lupus-like autoimmune disease in mice (Liu et al., 2006). In addition, TLR9 or TLR3 engagement has been shown to stimulate autoreactive B cells to secrete antibody (Ding et al., 2006). Overexpression of B cell–activating factor of the tumor necrosis factor family (BAFF) promoted a

The Rockefeller University Press $30.00
J. Exp. Med. Vol. 206 No. 12 2641-2657
www.jem.org/cgi/doi/10.1084/jem.20091982

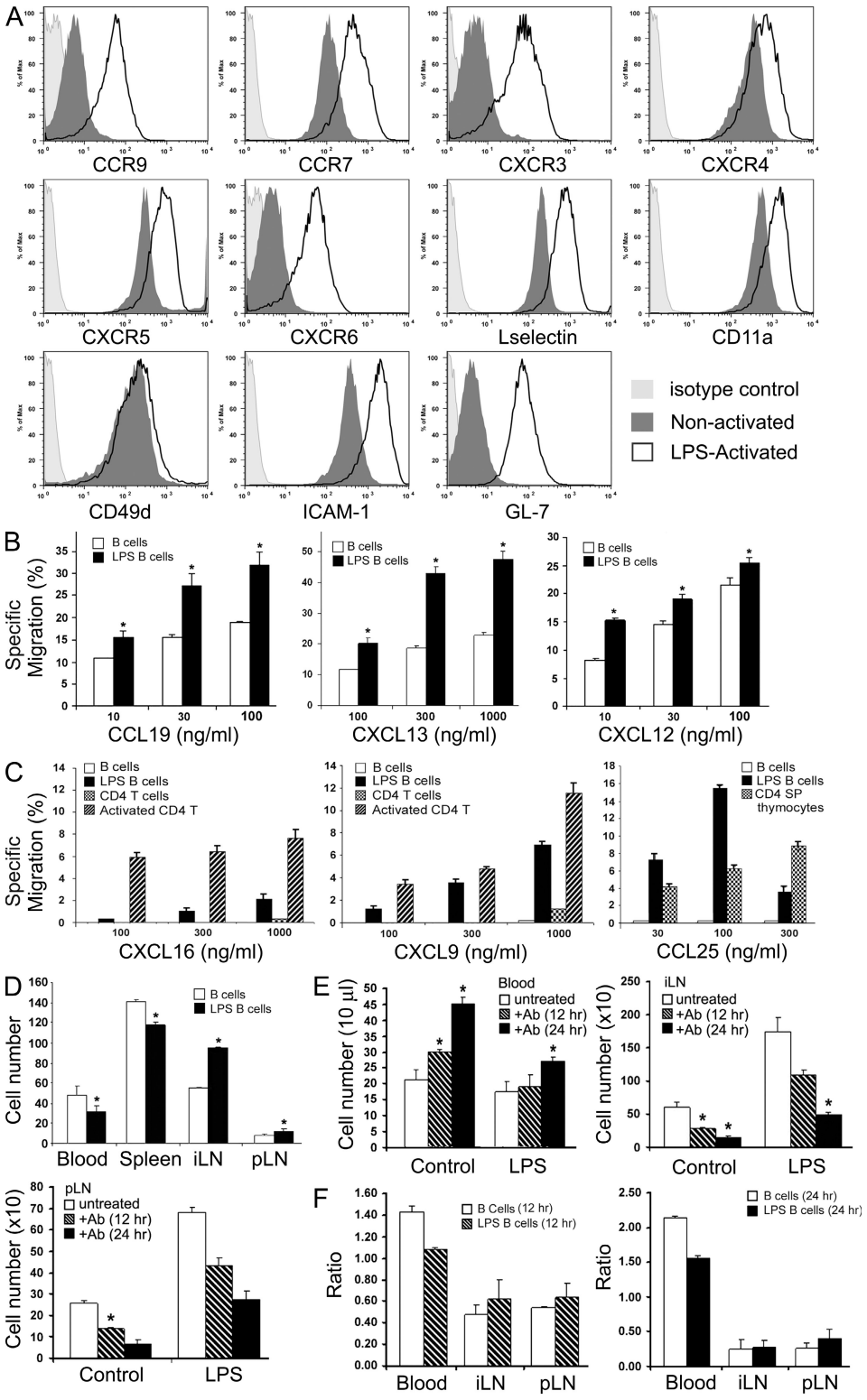

Figure 1. Signaling through TLR4 enhances B cell chemokine responsiveness. (A) Receptor expression. Splenic B cell was activated with LPS for 18 h or not activated. Stimulated B cell profiles, nonactivated B cell profiles, and isotype controls for indicated receptor are shown. A representative result is depicted from six performed experiments. (B) Chemotaxis assays. Stimulated and nonactivated B cell was subjected to 2 h of chemotaxis in response to CXCL12, CCL19, or CXCL13. The specific migration is shown. Results are mean and SE of sextuplet samples from six experiments (*, $P < 0.01$ vs. nonactivated B cell). (C) Chemotaxis to CXCL16, CXCL9, or CCL25. Results are mean and SE of sextuplet samples from six experiments. (D) Homing assay. Ten million differentially labeled LPS-activated and nonactivated B cells were intravenously transferred to recipient mice (six experiments each with three pairs

lupus-like disease in mice, which was independent of T cells but required B cell–intrinsic signals through the TLR adapter MyD88 (Groom et al., 2007). In addition, several studies have implicated dual BCR-TLR signaling in the pathogenesis of autoimmune diseases (Lanzavecchia and Sallusto, 2007). For example, DNA-containing Ig complexes activated autoreactive B cells to produce antibodies against self-IgG (Leadbetter et al., 2002) and, in $MRL^{lpr/lpr}$ mice, B cells that recognized self-IgG_{2a} depended on endogenous TLR ligands to trigger their expansion and differentiation to Ig secretion (William et al., 2002; Herlands et al., 2008).

A hallmark of many autoimmune diseases is the formation of ectopic and excessive numbers of germinal centers (Luzina et al., 2001; Hsu et al., 2008). Germinal centers are a site where B lymphocytes undergo clonal expansion, class switch recombination, antibody gene diversification, and affinity maturation (Liu et al., 1989; Jacob et al., 1991; MacLennan, 1994). TLR signaling has also been linked to germinal center formation. Injection of the TLR4 ligand LPS into the foot pad of mice induced the formation of new LN follicles and germinal centers (Horie and Hoshi, 1989). Immunization with DNP-LPS, which engages both DNP-specific antigen receptors and TLR4, initially decreased cell proliferation within preexisting germinal centers, which was followed by increased germinal center cell proliferation (Goodlad and Macartney, 1995). In addition, after murine gammaherpesvirus 68 infection, $MyD88^{-/-}$ B cells failed to become activated and to enter into germinal centers (Gargano et al., 2008).

Despite the importance of TLR signaling in regulating human and mouse B cell function and its linkage to autoimmunity, the impact of TLR signaling on the trafficking of human and mouse B cells has received little recent attention. One study examined the distribution in recipient mice of transferred radiolabeled B cells, stimulated in vitro with LPS or not, and concluded that LPS stimulation had little impact on B cell trafficking (Freitas and de Sousa, 1976). Since that study, much has been learned about how B lymphocytes traffic into and within lymphoid organs. Naive and memory B cells enter LNs from the circulation by crossing high endothelial venules, whereas memory B cells can also enter via afferent lymphatics (Cyster, 2005). Once within LNs, most B cells rapidly localize in the LN follicle. Intravital two-photon laser-scanning microscopy (TP-LSM) of mouse LNs has shown that follicular B cells move with an mean velocity of 6 μm/min along the processes of follicular DCs (FDCs; Miller et al., 2002; Han et al., 2005; Bajénoff et al., 2006). CXCL13 associated with the FDCs fuels B cell motility in the follicle. B lymphocytes from mice that possess B cells hyperresponsive or hyporesponsive to chemokines move faster or slower, respectively, than do wild-type B cells (Han et al., 2005). Follicular B cells that encounter their cognate antigen upregulate CCR7 expression and migrate to the B-T boundary to receive T cell help (Reif et al., 2002; Okada et al., 2005). This leads to B cell proliferation and differentiation into extrafollicular plasmablasts or to the seeding of germinal centers, which produce memory B cells and plasmablasts.

This study examines the consequences of TLR4 activation on mouse B cell chemokine responsiveness, lymphocyte trafficking, in vivo proliferation, and the behavior of the activated B cells within LNs. Direct visualization of the TLR4-activated B cells within LN follicles of live mice using TP-LSM demonstrated B–B cell interactions and the recruitment of the TLR4 ligand–exposed cells into the dark zones of germinal centers present in LNs. Many of the transferred TLR4-activated cells persist in mice and expand within the memory and plasma cell compartments. The implications of these observations are discussed.

RESULTS

TLR4 stimulation enhanced the B lymphocyte migratory program

We used flow cytometry to examine the effects of the TLR4 ligand LPS on the levels of homing and chemokine receptors. B cells stimulated with LPS increased their expression of the chemokine receptors CCR7 and CXCR5 and, to a lesser extent, CXCR4. In addition, the expression of CXCR3, CXCR6, and CCR9 were induced. LPS stimulation also increased the expression of the homing receptor L-selectin and proteins involved in cell adhesion, including CD11a and ICAM-1, although it did not alter CD49d. As expected, the activation marker GL-7 expression was enhanced by TLR4 stimulation (Fig. 1 A). Similar results were obtained when we compared freshly isolated B cells versus TLR4 ligand–stimulated B cells (Fig. S1 A). The LPS-exposed B cells responded better to CXCL12 (receptor CXCR4), CCL19 (receptor CCR7), and CXCL13 (receptor CXCR5) than did the unexposed B cells in chemotaxis assays (Fig. 1 B). The magnitude of the difference was greater for CXCL13 and CCL19 than for CXCL12. In addition, some of the LPS-exposed B cells acquired responsiveness to CXCL16 (receptor CXCR6), CXCL9 (receptor CXCR3), and CCL25 (receptor CCR9; Fig. 1 C). These differences existed whether we compared stimulated B cells to cultured B cells or to freshly isolated B cells (Fig. S1 B). Because of the importance

of mice; *, $P < 0.01$ vs. nonactivated B cell). 2 h after transfer, cells of the recipient mice were analyzed by flow cytometry. Shown are the actual number of transferred B cells found in blood (/10 μl), spleen (× 10^3 cells), iLN (× 10^2 cells), and pLN (× 10^2 cells). (E) LN transit assay. 10 million differentially labeled LPS-treated B cells and nontreated B cells were intravenously transferred (six experiments each with three pairs of mice; *, $P < 0.01$ vs. nonactivated B cell). 100 μg/mouse of anti–L-selectin antibody was injected intravenously 2 h after transfer. Control mice were injected with PBS (white bars) and analyzed immediately. Cells were isolated from the indicated sites and analyzed by flow cytometer at 12 h (shaded bars) and 24 h (black bars) after antibody injection. (F) Ratios. The ratios between 12 h of antibody, 24 h of antibody, and PBS-treated control groups are shown from the data in E. Error bars indicate means ± SEM each with three pairs of mice in six experiments.

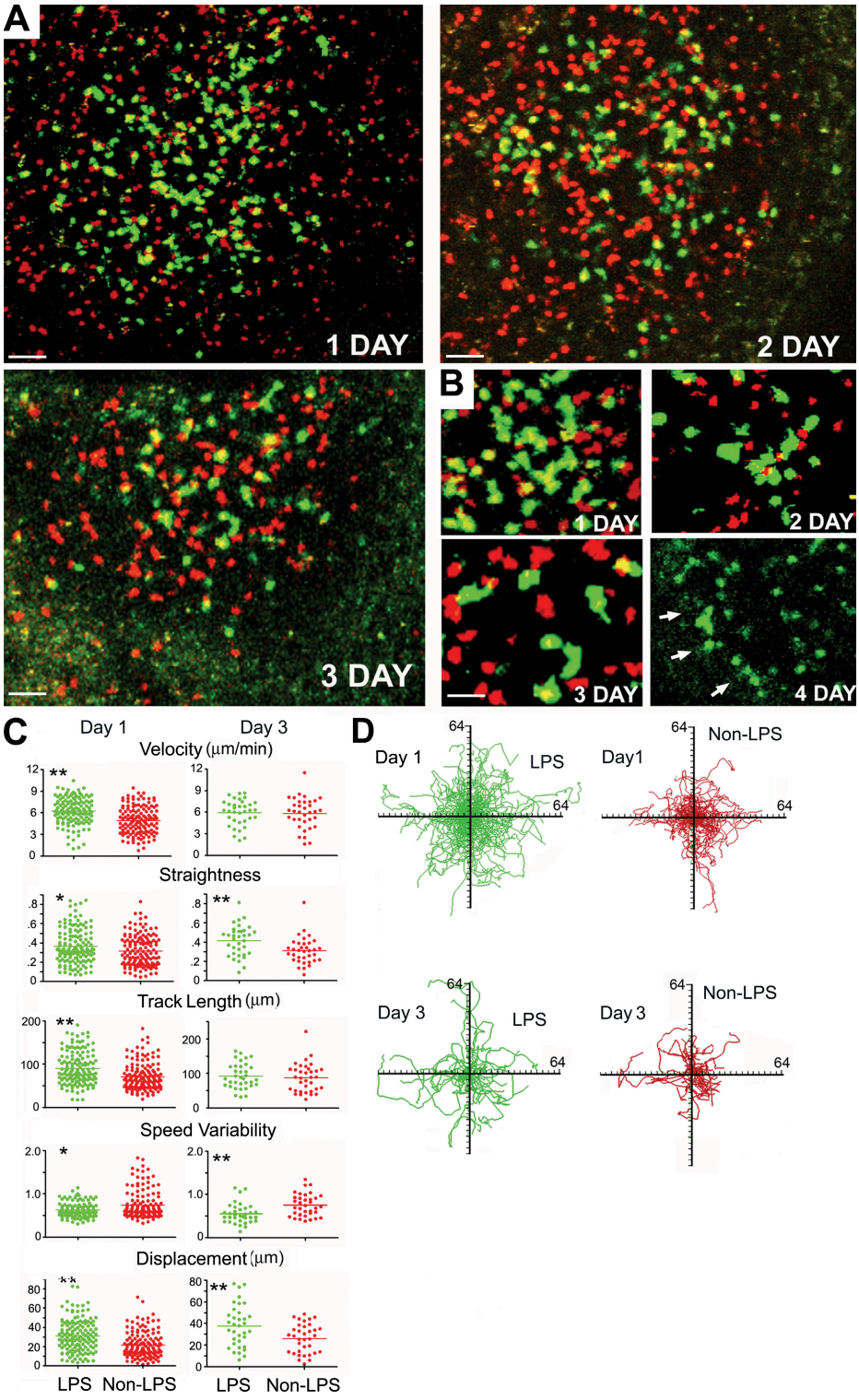

Figure 2. Comparison of TLR4 ligand–exposed or nonexposed B cells in the iLN by intravital TP-LSM. (A) Imaging. Labeled LPS-activated and control B cells were transferred to recipient mice and the iLN was imaged various days after transfer. A maximum intensity projection (MIP) of a 33-μm image stack shows LPS-activated B cells (green) and nontreated B cells (red). Bars, 50 μm. (B) Zoomed images. An MIP 4× zoom is shown of days 1–3. The day-4 data were obtained using CFSE-labeled and transferred LPS-activated B cells. Arrows point to LN follicle edge. Bar, 12.5 μm. (C) Motility parameters. Each data point represents a single cell and green and red bars indicate mean values (*, $P < 0.05$; **, $P < 0.01$). (D) Tracks. Superimposed 20-min tracks of randomly selected cells of indicated types in the x, y plane setting the starting coordinates to the origin. Data are from the analysis of four recipient mice at the indicated times. The experiment was done three times with similar results.

of $G_{i\alpha 2}$ and Rgs1 in regulating the output from chemokine receptor engagement (Moratz et al., 2004; Han et al., 2005; Hwang et al., 2007), we also checked the effect of LPS exposure on their expression. LPS stimulation increased *Gnai2* expression, which will augment chemokine receptor signaling, and reduced *Rgs1* expression, which should have the opposite effect, providing another reason why these cells exhibit strong chemotactic responses (Fig. S1 C). To test whether these changes translated into improved LN homing, we differentially labeled the TLR4 ligand–treated and control B cells and transferred them intravenously to recipient mice. 2 h later, we harvested LNs and spleen and sampled the blood of the recipient mice. We recovered ∼40% more TLR4-stimulated B cells from the LNs than from control cells and slightly fewer cells from the blood and spleen (Fig. 1 D).

Next, we determined whether the TLR4 ligand exposure affected LN transit time by transferring B cells previously cultured with LPS, or not, to recipient animals and, 2 h later, treating the mice with L-selectin antibody, inhibiting further entrance of B cells into the LNs. We harvested the popliteal LNs (pLNs) and inguinal LNs (iLNs) and sampled the blood either 12 or 24 h later (Fig. 1 E). The ratio between the numbers of cells in the LNs from the L-selectin–treated mice at 12 and 24 h versus those in the nontreated mice at 2 h is related to the mean transit time of the cell population. Surprisingly, the results showed only a slight enhancement in the retention of the stimulated B cells compared with the nonstimulated cells at 12 h, and by 24 h there was little difference (Fig. 1 F). Because we only examined the egress of those cells that had entered into the LNs within 2 h of transfer, our analysis is biased toward those cells that rapidly accessed LNs.

TLR4 ligand exposure changed the migratory behavior of B cells in the LN follicle

To investigate the migration dynamics of TLR4-stimulated B cells, we transferred differentially labeled LPS-stimulated or nonstimulated B cells into recipient mice. At various times after transfer, we visualized and tracked the movement of the cells by imaging them in the iLN intravitally using TP-LSM (Fig. 2, A and B). At 1 d after transfer, both B cell populations had localized in the LN follicle; however, the TLR4 ligand–exposed B cells (Fig. 2, A and B, green) tended toward the follicle center. Readily distinguishable from the nonactivated cells (Video 1, red), the larger TLR4-stimulated B cells often displayed a highly polarized morphology (Video 1, green). At days 2 and 3 after transfer, the stimulated B cells (Fig. 2 A, green) maintained their preference for the follicle center (Fig. S2) and continued to exhibit morphological differences from the nonactivated cells (Fig. 2 A, red). At later time points, we transferred CFSE-labeled B cells that were either nonactivated or TLR4 stimulated into different mice. 4 d later we separately imaged them. As we had observed at earlier time points, the non-TLR4 ligand–exposed cells remain uniformly distributed throughout the follicle (not depicted); however, the TLR4-stimulated cells no longer showed a preference for the center of the follicle and many cells lined up along the follicle edge (Fig. 2 B, green).

Tracking individual cells revealed that, on average, the TLR4 ligand–exposed B cells moved slightly faster than did the control B cells at 24 h; however, at 48 and 72 h after transfer the difference was negligible (Fig. 2 C and not depicted). It is of note that a small portion of the TLR4 ligand–exposed B cells (∼5%) exhibited an extreme polarized morphology with a long thin uropod, often with a length of two or three cell bodies, rather like a kite with a tail. At each of the time points examined the stimulated B cells moved slightly straighter, with less speed variability, and with a greater mean displacement than the nonstimulated cells (Fig. 2 C and not depicted). The greater displacement is readily visualized by plotting an equal number of randomly selected individual tracks from the same origin (Fig. 2 D).

Within the LN follicle, some of the TLR4 ligand–exposed B cells formed transient clusters of highly interactive cells. The clusters, which were often composed of five or more cells, persisted for as long as 10 min. Individual frames from the intravital imaging of transferred B cells present in the iLN of the recipient mouse are shown in Fig. 3 A and Video 2(green). Highlighted over the first 7 min is a cluster of five to seven B cells, which showed extensive cell–cell interactions (Fig. 3 A, top). After ∼8 min, the cluster disappeared and another cluster of B cells appeared just above the previous cluster. Again composed of five to seven B cells, the cluster lasted for ∼8 min and then began to dissipate. An example of a B cell with a long uropod is shown in Fig. 3 A (22:30). Another set of previously stimulated B cells tracked over a 15-min period 48 h after transfer is shown in Fig. 3 B. To determine the number of interactions and the duration of the interactions, we tracked the two populations 48 h after transfer. We found that, on average, the TLR4 ligand–exposed B cells had twice as many contacts, which lasted 70% longer on average than did the control B cells (Fig. 3 C). Although many of the interactions between the stimulated B cells appeared to be organized around specific sites in the LN follicle, the cells also exhibited an apparent attraction for each other (Fig. 3 D). They sometimes sped up before an interaction occurred, and during the interaction the cell velocities usually declined. In some instances, one cell reversed its direction after an interaction with another cell or, more frequently, it paused, which could be recognized by a loop in the track. Fig. 3 E shows the tracks of 18 TLR4 ligand–exposed B cells randomly chosen after selecting cells that remained within the imaging volume a minimum of 10 min. All but one of the cells had at least one interaction with another B cell. Graphs of the instantaneous velocities of two interactive LPS-exposed B cells are shown in Fig. 3 F.

TLR4 stimulation triggered a rapid expansion of B cells in vivo and some cells adopted a germinal center phenotype

The number of visible TLR4-stimulated B cells versus the nonstimulated B cells declined within 2–3 d after transfer. This could represent a decrease in the number of cells within the LNs or a dilution of the fluorescent dye in the TLR4-stimulated B cells as a consequence of cell division. To test whether the B cells proliferated in vivo, we transferred CFSE-labeled

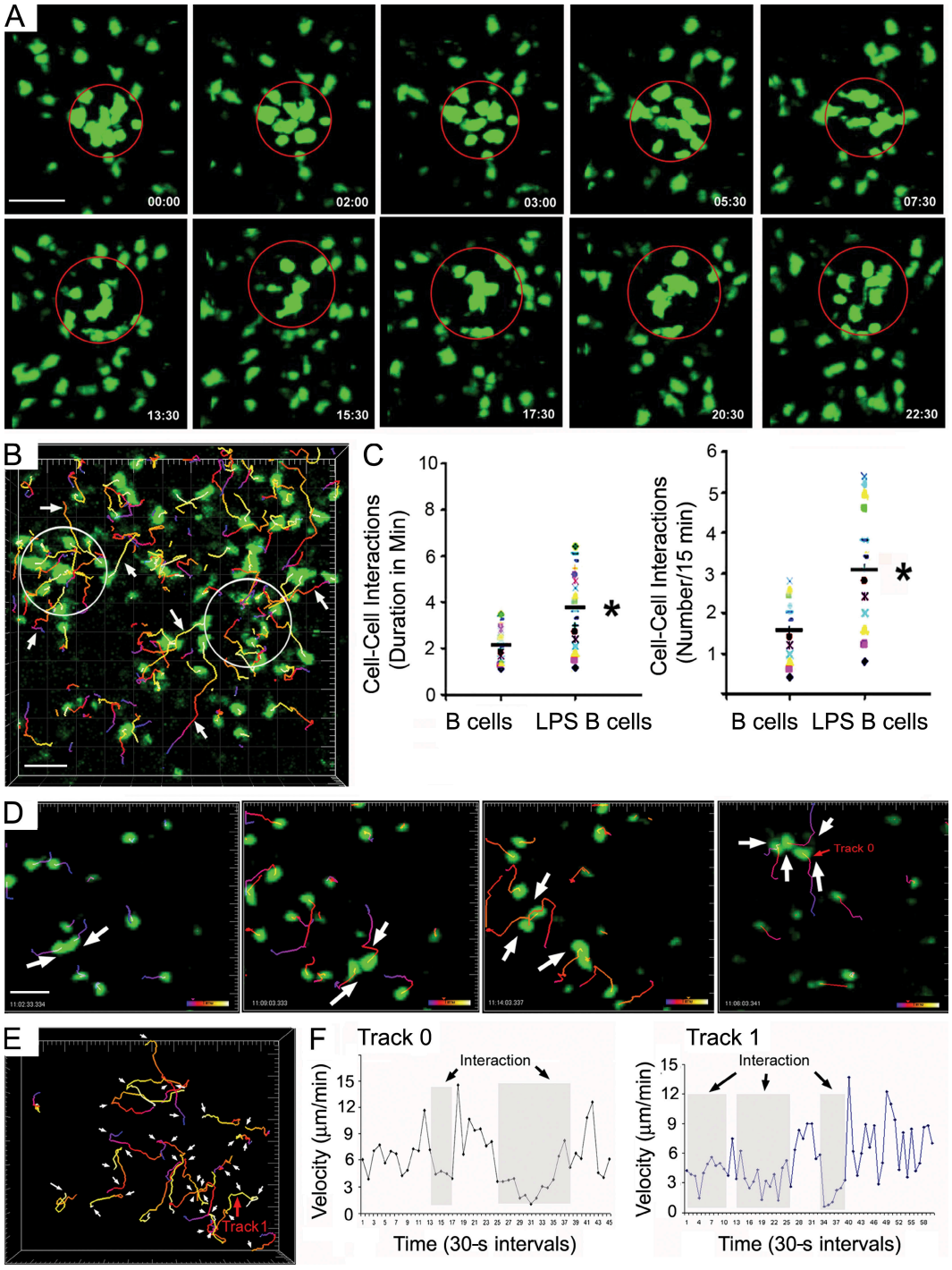

Figure 3. TLR4 ligand exposure triggers extensive B cell interactions in the LN follicle. (A) B cell clusters. MIP from TP-LSM of TLR4-stimulated B cell clusters (red circles) 1 d after transfer. Two separate regions (top and bottom) are shown. Bar, 20 µm. (B) Tracking clustered B cells. MIP and tracks of TLR4-stimulated B cell (green) 48 h after transfer. White circles indicate highly interactive cells and the time colored tracks (red, blue, and yellow) show movement of the TLR4-stimulated B cells over 20 min. Arrows point to several representative tracks. Bar, 20 µm. (C) Quantification of cell–cell interactions. The durations in which LPS-activated B cells contacted other activated B cells or nonstimulated B cells contacted other nonstimulated B cells are shown (left). Each cell was tracked for 15 min and the number of interactions is shown (right). Black bars indicate mean values (*, $P < 0.05$). (D) B cell–B cell interactions (arrows). MIPs of intravital TP-LSM of TLR4-stimulated B cells 72 h after transfer in the iLN. Image spaces are 130 × 115 × 33 µm (first and second) and 130 × 130 × 33 µm (third and fourth). Individual cells were tracked every 30 s for 30 min and their previous 20 positions are indicated by a dragon tail. Three frames from two sets of imaging data showing colliding LPS-stimulated B cells at various time points during the imaging. Track 1 is further analyzed in F. Bar, 20 µm. (E) Tracking interacting B cells. Tracks of TLR4-stimulated B cells 72 h after transfer. Imaging space is 240 × 190 × 33 µm. Individual tracks were sorted by duration and the top 18 of 60 tracks were selected. Interactions with other TLR4-stimulated B cells (both selected

cells and counted the number of recovered cells and analyzed their CFSE expression profile control (Hawkins et al., 2007; Quah et al., 2007). We recovered more TLR4 ligand–exposed B cells than control cells in the spleen, iLN, and pLN at days 2, 3, and 4 (Fig. 4 A). The number of nonstimulated cells remained relatively constant for the 5 d that we analyzed. The number of TLR4-stimulated B cells peaked at day 3 in the spleen and at day 4 in the LN. The CFSE profiles of the cells recovered from the spleen, popliteal, and iLN showed that some of the B cells exposed to LPS 5 d previously, which was 4 d after transfer, had significantly diluted their levels of CFSE, which is consistent with ongoing proliferation (Fig. 4 A and not depicted). This contrasted with the day-4 control B cells harvested from the spleen and LN, which had not diluted their CFSE.

To verify these results and to provide additional phenotyping data, we analyzed the cell recovery and CFSE profiles of TLR4 ligand–exposed CD45.1 B cells transferred into CD45.2 mice. Besides checking the transferred cells in the LNs and spleen, we also examined their presence in bone marrow. Compared with the initial experiments, we found a more marked expansion of the TLR4 ligand–exposed B cells. This is presumably the result of an inability to recognize some of the transferred cells in the first experiment because of dye dilution. Using CD45.1-marked cells, we observed an ∼40-fold increase in the number of cells between days 1 and 7 in the spleen, a 15-fold increase in the LN, and a twofold increase in the bone marrow (Fig. 4, B–D). Again many of the transferred cells markedly diluted their CFSE expression. We recovered $B220^{+}IgD^{high}$ and $B220^{+}IgD^{low}$ B cells from all three sites. The $B220^{+}IgD^{high}$ bone marrow cells recovered 3 d after transfer had not diluted their CFSE to the same degree as the $B220^{+}IgD^{high}$ B cells recovered from the spleen and iLN. We also found that a portion of the cells had adopted a germinal center B cell phenotype being $IgD^{low}GL7^{+}Fas^{+}$. Surprisingly, we also found these cells in the bone marrow. By day 9 after transfer the number of recovered cells declined, suggesting that some of the cells had died, although the numbers of $IgD^{low}GL7^{+}Fas^{+}$ cells remained relatively stable in the spleen and LN.

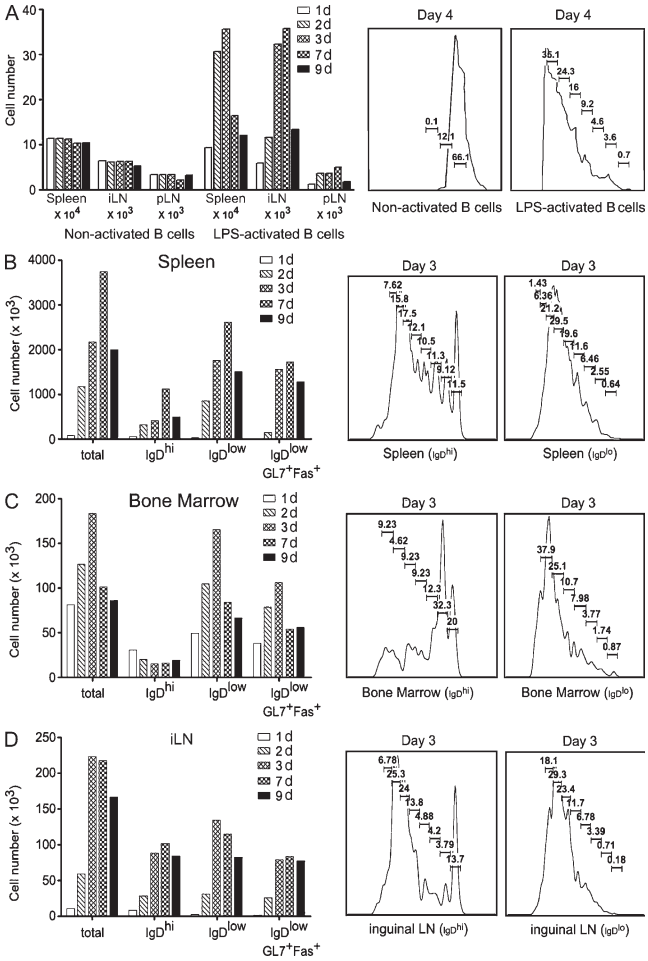

Figure 4. TLR4 ligand–exposed B cells proliferate in vivo and some adopt a germinal center phenotype. (A) Recovered cell numbers and CFSE profiles of nonstimulated and LPS-stimulated B cells. 10×10^6 cells were labeled with CFSE and transferred intravenously to different recipient mice. At the indicated days, the total number of viable CFSE-labeled cells recovered from the spleen, iLN, and pLN were determined (left). The CFSE profiles of the recovered splenic cells are shown, along with the percentage of cells that divided (right). Data from five recipient mice that received non-activated B cells and five that received LPS-activated B cells. (B–D) Recovery and phenotype of cells recovered from spleen, bone marrow, and iLN after transfer of LPS-stimulated CD45.1 B cells into CD45.2 mice. Number and phenotype of the recovered CD45.1 cells (left) and CFSE profiles of the CD45.1 cells recovered at day 3 after transfer (right) are shown. Data are from the analysis of five recipient mice that received LPS-activated B cells.

Recruitment of TLR4-activated B cells into ongoing germinal center reactions

For several reasons, it is of interest to determine whether LPS-activated B cells joined ongoing germinal center reactions. Recent imaging studies had revealed that follicular B cells can enter into the light zone of germinal centers (Schwickert et al., 2007), and we had noted that some of the LPS-stimulated B cells adopted a germinal center phenotype in vivo. Therefore, we transferred fluorescently labeled TLR4 ligand–exposed B cells into a mouse previously immunized with hen egg lysozyme (HEL) and examined the location of the transferred cells by intravital TP-LSM. Within the iLNs of immunized mice, we found several large clusters of B cells which were significantly larger than those we had observed previously (Fig. 5 A, top left). To determine the location of the cell clusters in relation to germinal centers, we injected a labeled FDC-M2 monoclonal antibody subcutaneously the day before imaging.

and nonselected) in the imaging space are indicated with arrows. Track 2 is further analyzed in F. (F) Velocity profiles. Instantaneous velocities of two tracks from TLR4-stimulated B cells are shown. Cell–cell interactions are indicated by shading. The tracks are from D and E. Imaging data shown is from the analysis of three recipient mice.

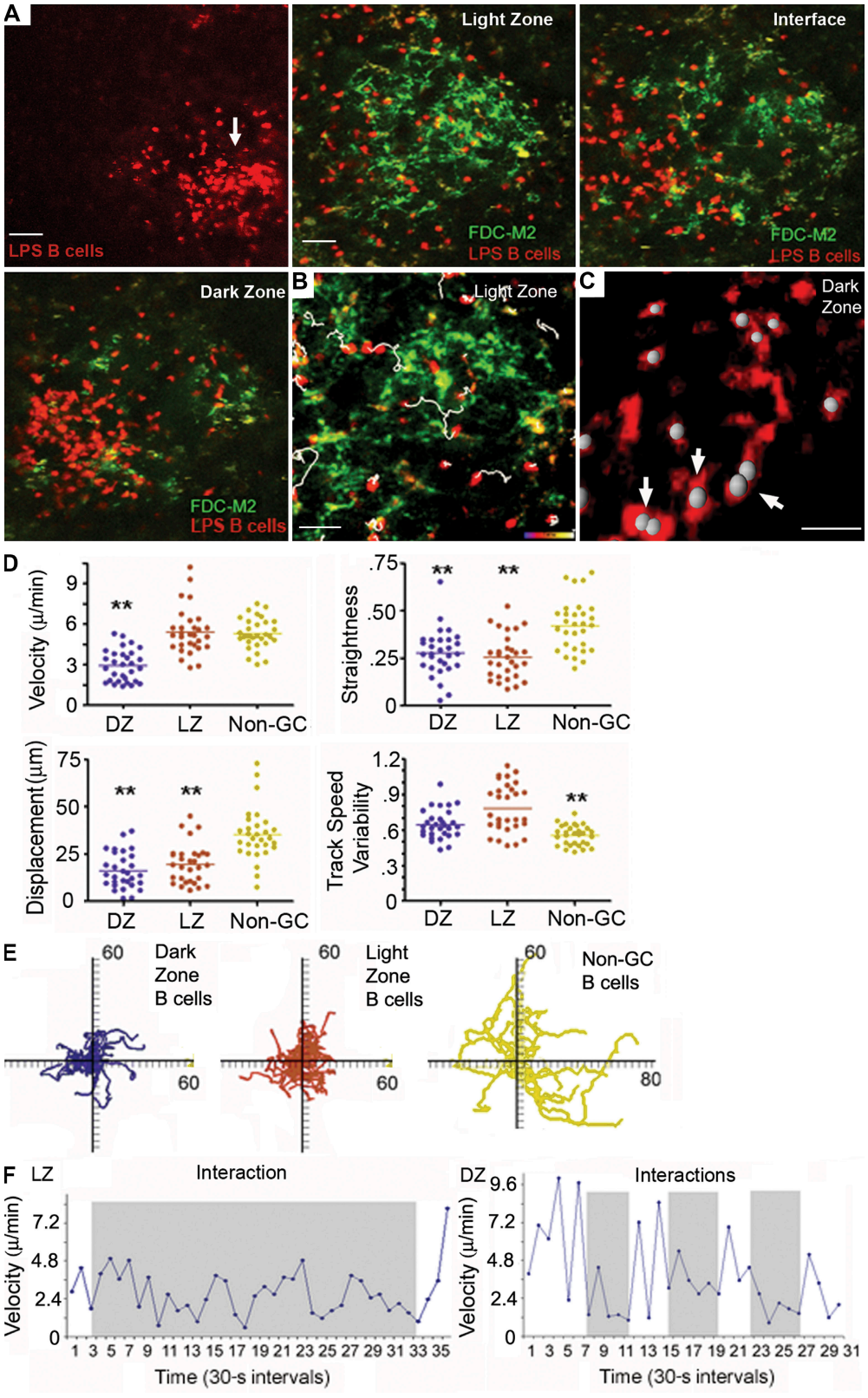

Figure 5. TLR4 ligand–treated B cells enter ongoing germinal center reactions and focus in the dark zone. (A) Germinal center imaging. MIPs of transferred TLR4-stimulated B cells (transferred 2 d before imaging) in iLN of mice immunized 1 wk previously with HEL. The top left shows a cluster of the TLR4-stimulated B cells (arrow) 1 wk after immunization. Also shown are images of TLR4-stimulated B cells in the light zone region, at the interface dark zone–light zone region, and in the dark zone region of the germinal center (bottom). Location of the cells defined by FDC-M2–positive cells were

FDC-M2 recognizes C4 deposited on FDCs, which densely pack the light zone region of germinal centers (Taylor et al., 2002). The light zone contains B cells that are termed centrocytes, which are the descendents of rapidly proliferating dark zone B cells known as centroblasts. In the absence of immunization we observed scattered sites of FDC-M2 staining in the LN follicle (unpublished data). After immunization, we observed a strongly FDC-M2–reactive region in the LN follicle, which is consistent with a germinal center light zone (Fig. 5 A, top center). Scattered among the FDC-M2–positive cells were TLR4 ligand–exposed B cells (Video 3). Imaging deeper into the follicle, we noted increasing numbers of B cells and, finally, a cluster of B cells in a location consistent with the dark zone (Fig. 5 A, top right and bottom left; Video 4). The TLR4 ligand–exposed B cells within the light zone region moved sequentially from one FDC to another. The migratory paths of the B cells in the light zone from one experiment are shown in Fig. 5 B. The B cells in the dark zone remained largely confined to that region and exhibited frequent B–B cell interactions (Fig. 5 C). In the dark zone, cells moved slower than they did in the light zone or outside the germinal center. The tracks of the light zone and dark zone B cells had reduced displacements and decreased straightness compared with the follicular but nongerminal center cells (Fig. 5, D and E). Plotting the instantaneous velocities of the light zone B cells that interacted with FDCs and dark zone B cells that interacted with each other revealed that the B cells slowed when they interacted with another cell (Fig. 5 F). We confirmed the location of the transferred LPS-stimulated cells in the dark zone of germinal centers by immunohistochemistry (Fig. S3).

TLR4 ligand–exposed B cells competed efficiently with antigen-specific B cells for entrance, divided within the dark zone, and many remained within the dark zones of splenic germinal centers

Entrance into the dark zone of germinal centers has been thought to be restricted to antigen-activated B cells, whereas non–antigen-specific B cells can only visit the light zone (Schwickert et al., 2007). To directly compare antigen-specific B cells and TLR4 ligand–exposed B cells in their ability to access the dark zone region of preexisting germinal center, we transferred equal numbers of differentially labeled LPS-exposed C7Bl/6 B cells and HEL-transgenic B cells into recipient mice that had been immunized 10 d earlier with HEL. Imaging the iLN of recipient mice 2 d after transfer revealed that in all the visible germinal centers, the number of TLR4 ligand–stimulated B cells far exceeded the number of antigen-specific B cells in the dark zone region (Fig. 6 A and Video 5). This, in part, reflects the better efficiency with which the TLR4-stimulated B cells enter LNs, but tracking individual TLR4-stimulated and transgenic B cells indicated that relatively few antigen-specific B cells had entered the dark zone at this time point (Fig. 6 A, right).

In the course of imaging the TLR4-stimulated B cells within the dark zone of germinal centers we noted numerous dividing cells (Video 6). Images captured during intravital microscopy showed three cells in the dark zone that divided during a 45-min imaging session. The individual cells are highlighted (Fig. 6 B, left). Serial zoomed images show the cell outlined in the yellow box dividing (Fig. 6 B, right). The cell has rounded up in the 9:00-min image and begins to divide in the 28:00-min image. The daughter cells remained adjacent for the duration of the imaging period.

Next, we determined whether the TLR4 ligand–exposed B cells entered splenic germinal centers. To do so, we transferred TLR4-stimulated GFP-positive B cells and CMF_2HC-labeled nonstimulated B cells to recipient mice immunized 7 d previously with HEL and injected the mice with fluorescently labeled FDC-M2 antibody (red). 4 d later, we prepared thick frozen sections of the spleens of recipient mice and examined the location of the transferred cells by TP-LSM. We found that the injected FDC-M2 antibody allowed us to identify the germinal centers in the splenic section. The dark zones were defined on the basis of their location in relation to the FDC-M2–staining cells. We found numerous germinal centers in which the previously TLR4-stimulated B cells had accessed and accumulated within the dark zone regions. In contrast, the control cells failed to access the dark zones of germinal centers (Fig. 6 C).

TLR4-stimulated B cells augmented an antigen-stimulated antibody response and persisted after transfer in the bone marrow, spleen, and LN

To examine whether TLR4 ligand–exposed cells can augment an ongoing immune response, we immunized CD45.2 mice with HEL and, 1 wk later, transferred either TLR4 ligand–stimulated CD45.1 B cells or nonstimulated CD45.1 B cells.

revealed by Alexa Fluor 488–labeled FDC-M2 injected 1 d before imaging. Bars, 50 µm. (B) Tracking. TLR4-stimulated B cells within the germinal center light zone. TLR4-stimulated cells imaged intravitally (FDC-M2, green; TLR4-stimulated B cell, red) were tracked for 20 min. Tracks (white) are from those cells that remained in the imaging space for at least 10 min. Bar, 50 µm. (C) Dark zone interactions. A single slice is shown from intravital TP-LSM showing the location of TLR4-stimulated B cells in the dark zone region. The centers of each cell are indicated with a gray ball. Three pairs of interacting B cells are indicated with white arrows. In one pair the centers were superimposed. Bar, 20 µm. (D) Motility parameters. Cell motilities in light zone (LZ), in dark zone (DZ), and outside of the germinal center (Non-GC) were determined. Each data point represents a single cell and blue, red, and yellow bars indicate mean values (**, $P < 0.05$). (E) Tracks. Shown are superimposed tracks of TLR4-stimulated cells of each indicated type in the x, y plane setting the starting coordinates to the origin. Tracks of 30 cells in the indicated sites tracked for 15 min of a 20-min imaging experiment. (F) Velocity profiles. Magnitudes are shown of the instantaneous velocities of TLR4-stimulated B cells in the light zone and the dark zone. An interaction with another cell is indicated by shading. Experiments were performed five times using multiple recipient mice.

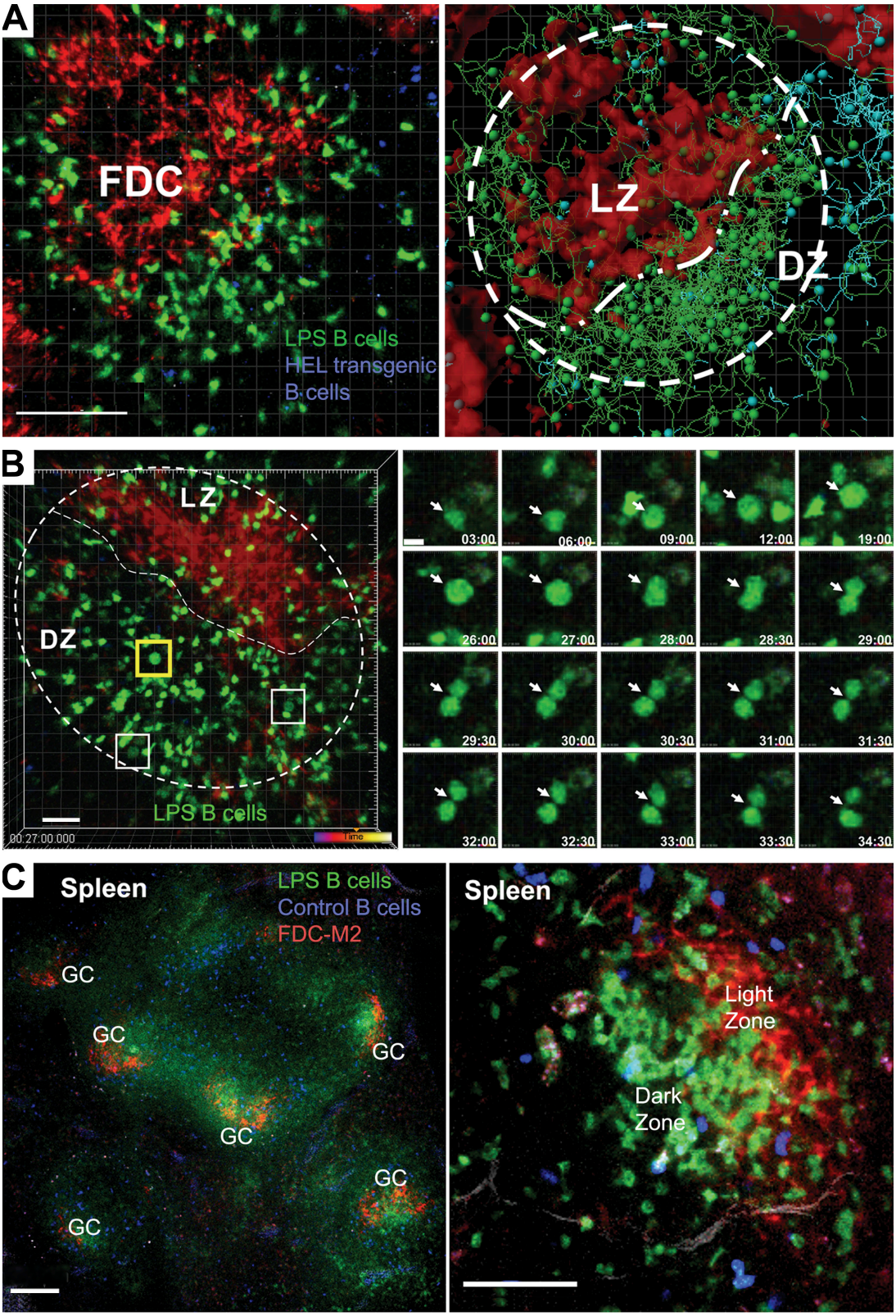

Figure 6. TLR4 ligand–stimulated B cells that have entered the dark zone can compete efficiently with antigen-specific B cells for dark zone entrance and can divide and persist in the spleen. (A) Competition. Fluorescently stained HEL-transgenic B cells (blue) and LPS-pulsed B cells (green) were adoptively transferred into a recipient mouse immunized 10 d previously with HEL. FDC-M2 antibody was injected 1 d later, and the next day intravital TP-LSM intravital imaging was performed. An MIP image from TP-LSM intravital imaging of the iLN is shown on the left. The tracking of

We measured specific Ig response in serum samples collected 3 wk after the cell transfer and again 10 d after boosting with HEL. We found that the addition of the TLR4 ligand–stimulated cells increased the HEL-specific IgM response 50% and the HEL-specific IgG1 response 15% compared with nonstimulated cells. The transfer of TLR4-activated B cells increased the HEL-specific IgG2a and IgG2b responses at day 28 (~25%) but did not enhance the levels achieved after re-exposure to antigen (Fig. S4). To determine the location of the transferred cells after antigen boosting (day 38 after transfer), we performed immunohistochemistry using either CD35 and CD45.1 or MAdCAM-1 and CD45.1. CD35 allows distinction of the B and T cell zones, whereas MAdCAM-1 delineates the marginal sinus. We found numerous transferred CD45.1 cells in the spleens from mice that had received TLR4-stimulated B cells, which contrasted with the relative paucity in the spleens of mice that had received the non–TLR4-stimulated CD45.1 cells (Fig. 7). Many of the previously stimulated CD45.1 cells resided in the B cell follicles and in the marginal zones of the CD45.2 mice (Fig. 7). In addition, we found CD45.1 cells in ongoing germinal centers in the spleens of mice that had received an antigen boost 10 d previously. Approximately 30% of the splenic germinal centers contained CD45.2 cells. In some instances, the majority of the cells within a germinal center were of CD45.2 origin, whereas in others we detected only a few or no CD45.2 cells (Fig. S5).

We used one final approach to assess the persistence and fate of the transferred LPS-stimulated B cells: we transferred GFP-expressing B cells that had been stimulated, or not, into mice immunized 1 wk previously with HEL in one flank. 2 wk later the mice were boosted with HEL antigen at the same site, and 4 wk after the boost we collected bone marrow, iLN, and spleen to analyze the numbers and phenotypes of the recovered cells. Previous TLR4 stimulation enhanced the recovery of $B220^+$, $B220^+CD138^+$, $B220^+IgG1^+$, and $B220^{lo}IgG1^+$ cells from the spleens, LNs, and bone marrows when compared with the recovery of similar phenotyped nonstimulated B cells. For example, in the spleens we recovered 7-fold more $B220^+$, 2-fold more $B220^+CD138^+$, 10-fold more $B220^+IgG1^+$, and 2-fold more $B220^{lo}IgG1^+$ cells. In those mice that received LPS-stimulated B cells, we recovered fivefold more $B220^+$ and $B220^+CD138^+$ cells from the iLN on the immunized side as compared with the non-immunized side and 50-fold more $B220^+IgG1^+$-positive cells (Fig. 8). Together, these results indicate that the transfer of TLR4-stimulated B cells can augment the specific antibody response to thymus-dependent antigen, and some of the previously TLR4-stimulated B cells or their progeny can be recovered weeks later in the spleen, LN, and bone marrow.

DISCUSSION

The germinal center reaction generates memory B cells and long-lived plasma cells that produce antibodies with a high affinity for pathogens. This response helps eliminate persistent infections, provides protection against future encounters with the same or, in some instances, related pathogens, and helps to diversify the antibody repertoire. However, because of the complexity of this response, germinal centers are often a site of pathology. Many B cell lymphomas arise from germinal center B cells, germinal centers can generate autoreactive B cells, and excessive numbers and ectopic germinal centers often accompany autoimmune illnesses and chronic inflammatory conditions (Luzina et al., 2001; Aloisi and Pujol-Borrell, 2006; Klein and Dalla-Favera, 2008). In this study, we show that exposure to the TLR4 ligand LPS induced significant alterations in B lymphocyte trafficking and behavior within LNs. Surprisingly, in both LNs and the spleen previous exposure of B cells to LPS led to the recruitment of B cells into preexisting germinal centers, overcoming the restriction that limits the access of non–antigen-reactive B cells to the germinal center dark zone.

The evidence that exposure to a TLR4 ligand alters B lymphocyte trafficking is considerable. Flow cytometry results showed enhanced expression of CXCR3-6, CCR7, CCR9, L-selectin, CD11a, and ICAM-1, chemotaxis data showed enhanced responses to the cognate chemokines of these receptors, and homing data revealed a superior homing of the TLR4 ligand–treated B cells to LNs. In addition, LPS stimulation decreased the *Rgs1/Gnai2* ratio, which will augment chemokine receptor signaling. This contrasts with human bone marrow–derived DCs, where LPS stimulation increased the ratio (Shi et al., 2004). Somewhat surprisingly, we found that LPS activation did not significantly delay the transit time of B cells through the iLNs and pLNs. This was despite decreased *S1pr1* messenger RNA expression after LPS stimulation (unpublished data). Although those B cells exposed to LPS have an enhanced propensity to enter LNs, they are not confined to the LNs and spleen but, likely, continue to recirculate.

The behavior of the TLR4 ligand–treated B cells within the LN differed significantly from either antigen-activated or

LPS-stimulated and transgenic B cells is shown on the right. The location of the B cells at the beginning of the tracking is shown with a green (LPS stimulated) or blue (not stimulated) ball. Bar, 100 µm. (B) B cells dividing in the dark zone. MIP from intravital TP-LSM imaging of the dark zone of a germinal center showing three cells that divided during 20 min of imaging. White squares show three cells in the dark zone that divided during a 45-min imaging. Zoomed images from the TP-LSM imaging, which are focused on the cell outlined in yellow in the left, are shown on the right. The arrows indicate cell dividing. Bar: (left) 40 µm; (right) 50 µm. (C) Persistence in the spleen. TP-LSM images of cryostat sections of spleen. Fluorescently stained B cells (blue) and LPS-stimulated GFP-B cells (green) were adoptively transferred into the recipient mouse immunized 7 d previously with HEL. 4 d later, 10 µg of labeled anti–FDC-M2 antibody (red) was injected subcutaneously. The following day, spleen was collected, fixed, and cryostat sections prepared. The image on the left was acquired with a 10× lens and the image on the right was acquired with a 40× lens. GC, germinal center. Bar: (left) 100 µm; (right) 50 µm. The experiment was performed twice with similar results.

nonstimulated cells. Normally, B cells enter the LN follicle and distribute uniformly throughout, whereas antigen stimulation causes B cells to localize along the LN follicle border with the T cell zone (Okada et al., 2005). B cells stimulated in vitro with anti-IgM and transferred to recipient animals also localize along the B/T cell border (unpublished data). In contrast, the transferred TLR4-stimulated B cells localized away from the B/T cell border more in the center of the LN follicle. The distribution of antigen-activated B cells along the B/T border is caused, at least in part, by an increased CCR7 expression relative to CXCR5 promoting migration toward the CCR7 ligands in the T cell zone (Reif et al., 2002; Okada et al., 2005).

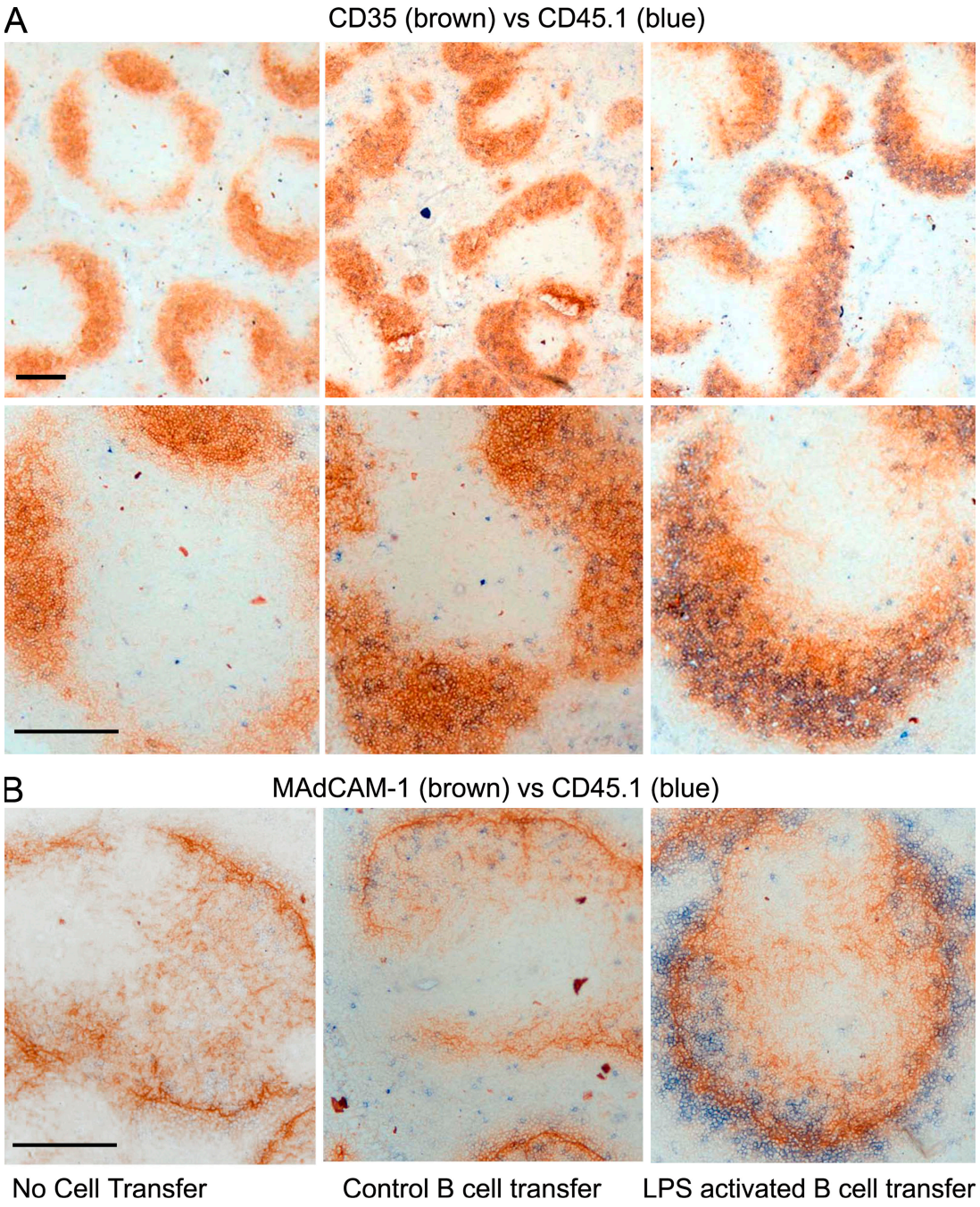

Figure 7. LPS-activated transferred B cells accumulate in the recipient spleens. (A and B) Transferred LPS-activated B cells are found in the B cell follicle and the marginal zone of the spleen. Three groups of five mice (6 wk old, C57BL/6 CD45.2) were injected subcutaneously on day 0 with 100 µg HEL in CFA. 15 million cells of LPS-activated or nonactivated B cells from C57BL/6 CD45.1 mice were injected intravenously to recipient mice on day 7. Mice were boosted on day 28 with 100 µg HEL antigen. On day 38, the mice were sacrificed and the spleens analyzed by immunohistochemistry to detect CD35 and CD45.1 (10× and 20×; A) and to detect MAdCAM-1 versus CD45.1 (20×; B). Bars, 100 µm. The experiment was performed with five mice with similar results.

Before transfer, the TLR4 ligand–stimulated B cells had increased both CCR7 and CXCR5 expression, although they exhibited a more exaggerated chemotactic response to CXCL13 than to CCL19. Although this may account for their positioning with the follicle, these cells also had increased their expression of CXCR3 and acquired responsiveness to CXCR3 ligand. Suggesting that this may be important, a recent microarray experiment demonstrated that FDC-enriched splenocytes expressed the CXCR3 ligand CCL10 in addition to CXCL13 and CXCL12 (Huber et al., 2005).

Both B cell–B cell contacts and B cell–stromal cell interactions affect the motility pattern of the TLR4-stimulated B cells within the LN follicle. They exhibited nearly twice as many interactions with their counterparts than did the nontreated control cells, and the mean duration of the interactions was nearly twice as long. Tracking individual cells reveals that many of the B–B cell interactions caused significant pausing or abrupt direction changes. At least a portion of the interactions between the TLR4 ligand–treated B cells are likely to be nonrandom. At later time points, the density of visible LPS-treated B cells within the imaging space was lower than the nontreated cells and the velocity profiles were similar, yet the treated B cells exhibited significantly more contacts. The increased interactions could arise from B–B cell communication potentially mediated by production of chemoattractants or by confinement of TLR4 ligand–exposed B cells by stromal cell interaction. Supporting the former explanation, several studies have shown that activated B cells produce chemokines (Schaniel et al., 1998, 1999).

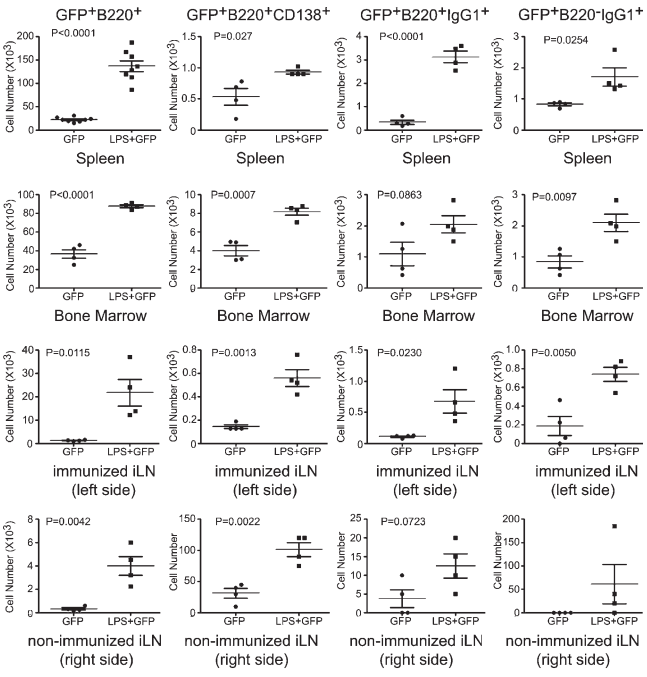

Figure 8. TLR ligand–exposed B cells differentiated into CD138 plasma and IgG1-positive B cell. LPS-activated or nonactivated B cells were prepared from GFP mice and transferred into mice immunized 1 wk previously with HEL in CFA. 21 d after immunization, mice were boosted with 100 µg HEL in PBS. 4 wk after boosting, spleen, iLN (immunized and nonimmunized side), and femurs (bone marrow) were removed, gently dissociated into single cell suspensions, and subjected to flow cytometry to analyze GFP, B220, IgG1, or CD138 as indicated. The data shown is mean ± SD from four recipient mice that received non–LPS-activated B cells and four recipient mice that received LPS-activated B cells. The horizontal bars indicate mean values.

Based on cell counting and CFSE dilution studies, many of the TLR4-stimulated B cells rapidly expanded after transfer; however, after the first week the numbers of recovered transferred cells began to decline. In another set of experiments using GFP-labeled cells, we recovered ∼10-fold more B220-positive cells from the spleen and LNs of mice 6 wk after transfer of LPS-stimulated B cells as compared with nonstimulated B cells. These data suggest that periodic exposure to TLR4 ligands may substantially skew the B cell populations in the spleen and LNs. This may arise both as a consequence of the proliferative potential of TLR4-stimulated cells and their ability to compete for survival signals as compared with nonstimulated cells.

Recent in vivo imaging of germinal centers revealed a dynamic open structure where follicular B cells frequently visited the FDC-rich germinal center light zone but not the germinal center dark zone (Schwickert et al., 2007). Within the dark zone, antigen-reactive B cells had a significantly decreased speed, increased cell volume, and greater confinement than did non–antigen-reactive B cells in the follicle (Allen et al., 2007; Hauser et al., 2007; Schwickert et al., 2007). Although not antigen activated, the LPS-exposed B cells readily entered the dark zone of ongoing germinal centers, where they divided and persisted. Similar to antigen-activated B cells in the dark zone, the TLR4 ligand–exposed B cells exhibited evidence of physical restriction. These results show that antigen activation is not a requirement for B cells to enter the dark zone. TLR4 engagement and subsequent B cell activation likely induces or up-regulates the expression of chemoattractant receptors that can recruit B cells into the dark zone. CXCR4 has been previously suggested as a possibility (Allen et al., 2004), although we observed only a modest increase in CXCR4 expression after LPS exposure. Within the dark zone, TLR4 ligand–exposed B cells will find themselves in an environment where they can proliferate, undergo class switching, and, perhaps, undergo somatic hypermutation. Treatment of B cells with LPS is known to increase expression of the enzyme activation-induced cytidine deaminase (AID; Muramatsu et al., 2000) and we verified that this was the case in our experiments (unpublished data). AID expression is necessary for the somatic hypermutation and Ig switch recombination that occurs within germinal centers (Muramatsu et al., 2000). However, although in vitro LPS stimulation is sufficient to trigger class switch recombination it does not induce mutations in Ig variable genes. Other signals, likely present within the dark zone, may alter AID activity allowing somatic hypermutation.

What is the fate of a dark zone germinal center B cell that lacks an antigen receptor reactive with the antigens that

elicited the formation of the germinal center? Those cells that enter relatively young or mixed germinal centers are likely to have a better chance of survival than those entering a well established germinal center already populated with high-affinity B cells. In younger germinal center, some of the LPS-exposed B cells may acquire antigen receptors that allow them to compete with antigen-activated B cells for survival signals. In fact, after antigen boosting we could find germinal centers that contained transferred cells. In addition, because lower affinity germinal center B cells tend to be shunted toward the memory B cell compartment (Paus et al., 2006; Benson et al., 2007; Tarlinton, 2008), feeding germinal center dark zones with randomly activated B cells could generate low-affinity memory B cells that would further diversify the antibody repertoire. Consistent with that possibility, we found that the addition of TLR4-stimulated B cells to previously immunized mice resulted in a significant increase in the number of $B220^{+}IgG1^{+}$ cells compared with the mice, which received nonstimulated cells. A large number of the TLR4-stimulated B cells localized in the marginal zone, a site known to accumulate memory B cells (Liu et al., 1988). However, because memory B cells can arise in the absence of germinal center formation, whether these cells previously visited a germinal center remains unknown (Anderson et al., 2007). Finally, a significant proportion of the TLR4 ligand–treated B cells that enter the dark zone may not receive survival signals and die, although engagement of TLR4 provides some survival signals not conferred by antigen activation (Souvannavong et al., 2004). In the setting of autoimmunity where B cell tolerance check points in the germinal center may have failed (Cappione et al., 2005; William et al., 2006), germinal center dark zones may be replenished by TLR-stimulated B cells, some likely to be autoreactive and perhaps even anergic. There the cells may find themselves in an environment that promotes their expansion and differentiation.

In conclusion, the observations and analyses reported here suggest that TLR4 signaling directs peripheral B cells to rapidly locate within LNs and the splenic white pulp. It likely does so by enhancing chemokine receptor expression, increasing the expression of L-selectin, and biasing the signaling pathway toward heightened responsiveness. Within the LN follicle, the TLR4 ligand–treated B cells exhibit behavior that is significantly different from nonstimulated or antigen-stimulated B cells. The TLR4-activated cells predominantly reside in the center of the LN follicle where they can directly interact with each other. The expansion of these cells in vivo suggests that these contacts may provide signals that help maintain the activated phenotype. If an LN follicle contains a germinal center, exposure to a TLR4 ligand will promote the entrance of stimulated B cells into the dark zone. TLR signaling may further fuel ongoing germinal center responses, providing a mechanism that augments the polyclonal expansion of the B cells which occurs after exposure to infectious agents and during the course of autoimmune illnesses.

MATERIALS AND METHODS

Mice. C57BL/6, B6.SJL-Ptprc^{a} Pepc^{b}/BoyJ, C57BL/6 (B6)-Tg(IghelMD4)4Ccg/J, and C57BL/6-Tg(UBC-GFP)30Scha/J mice were obtained from The Jackson Laboratory or Taconic. All mice used in this study were 6–12 wk of age. Mice were housed under specific pathogen-free conditions. All the animal experiments and protocols used in this study were approached by the National Institute of Allergy and Infectious Diseases Animal Care and Use Committee at the National Institutes of Health.

Cell culture. Splenic B cells were isolated by negative depletion using biotinylated antibodies to CD4, CD8, Gr-1 (Ly-6c and Ly 6G), and CD11c and Dynabeads M-280 Streptavidin (Invitrogen) as previously described (Hwang et al., 2007). The B cell purity was >95%. B cells were cultured in RPMI 1640 containing 10% FBS (Invitrogen), 2 mM L-glutamine, antibiotics (100 IU/ml penicillin and 100 μg/ml streptomycin), 1 mM sodium pyruvate, and 50 μM 2-mercaptoethanol. For the in vitro stimulation of B cell, B cells were treated or untreated with 1 μg/ml LPS (from *Escherichia coli* 055:B5; Sigma-Aldrich) overnight. The cells were cultured in T25 flasks at a concentration of two million cells/ml. Subsequently, the cells were collected and washed three times with PBS. The viability of the cells was determined by propidium iodide staining before analysis or cell transfer.

Flow cytometric analysis. TLR4-stimulated or nonactivated cell suspensions were stained with antibodies. Antibodies used were the following: biotin-conjugated antibody to CCR7 (BioLegend), anti-CXCR4, anti-CXCR5, anti-CD62L, anti-CD11a, anti-CD49d, anti-CD138, anti-GL7 (BD), and anti-ICAM-1 (BioLegend), FITC-conjugated anti-GL-7, anti-CD4, and anti-CD8 (BD), PE-conjugated anti-CCR9, anti-CXCR3, anti-CXCR6 (R&D Systems), anti-CD138, anti-CD4, anti-CD8 (BD), and IgD (eBioscience), PE-Cy7–conjugated anti-CD95, allophycocyanin-conjugated anti-B220 and anti-IgG1 (BD), Pacific blue–conjugated anti-B220, Alexa Fluor 647 anti–GL-7, and Alexa Fluor 750 anti-CD45.1. Streptavidin-PE and PerCP-Cy5.5 were obtained from BD. Data were collected on a FACSCalibur or CANTO II (BD) and analyzed with FlowJo software (Tree Star, Inc.). The CFSE dilution studies were performed according to a previously published protocol (Hawkins et al., 2007; Quah et al., 2007) and analyzed with FlowJo software.

Chemotaxis. Chemotaxis assays were performed using a transwell chamber (Costar; Corning) as previously described (Moratz et al., 2004). After being LPS activated or not, the B cells were washed twice, resuspended in complete RPMI 1640 medium, and added in a volume of 100 μl to the upper wells of a 24-well transwell plate with a 5-μm insert. Lower wells contained various doses of chemokines in 600 μl of complete RPMI 1640 medium. For chemotaxis with CXCL9 and CXCL16, splenic CD4 T cells were activated with 2 μg of anti-CD3 plus 10 ng/ml of recombinant mouse IL-2 for 24 h. CD4 single-positive thymocytes were used for some of the chemotaxis assays with CCL25. The numbers of cells that migrated to the lower well after either a 2 or 3 h incubation were counted using a flow cytometer. The LPS-stimulated B cells had a slightly higher basal migration in the absence of chemokine (~8 vs. 5%). Specific chemotaxis is the percentage of cells that migrated into the bottom chamber in the presence of chemokine minus the percentage of cells that migrated in the absence of chemokine.

RT-PCR. RNA was isolated with the TRIZOL reagent (Invitrogen) according to the manufacturer's instructions. Complementary DNA was synthesized from 1 μg RNA with the Omniscript RT kit (QIAGEN) with Omniscript reverse transcription according to the manufacturer's instructions. For PCR, 1 μl of the complementary DNA was placed in final volume of 50 μl containing HotStarTaq Plus Master Mix (QIAGEN) and RNase-free water and primers. The following primer pairs were used: β-actin, 5′-CCTAAGGCCAACCGTGAAAAG-3′ and 5′-TCTTCATGGTGCTAGGAGCCA-3′; *Rgs1*, 5′-GATCCCACATCTGGAATCTGG-3′and5′-GCTGTCGATTCTCGAGTATGG-3′; and *Gnai2*, 5′-CTCTAAAATGATCGACAAGAACCT-3′ and 5′-ACATCTTGAAGTGTAAGTCCTTGA-3′. The PCR amplifications

were performed with the following protocol: 95°C for 15 min initially, followed by 26–30 cycles of 1 min at 94°C, 1 min at 58 or 65°C, and 2 min at 72°C, and finally 1 cycle at 72°C for 10 min. The PCR products were separated by electrophoresis in 2% agarose and visualized by staining with ethidium bromide. For each primer pair, the number of PCR cycles was chosen to be in the linear amplification range.

Intravital two-photon microscopy. iLNs were prepared for intravital microscopy as previously described (Han et al., 2005). Cell populations were labeled for 15 min at 37°C with ∼2.5–5 μM of red cell tracker CMTMR, green cell tracker CMFDA, or blue cell tracker CMF_2HC (Invitrogen). 7–10 million labeled cells of each population in 200 μl of PBS were adoptively transferred by tail vein injection into ∼6–10-wk-old recipient mice. After anesthetizing the mice by intraperitoneal injection of 300 mg/kg Avertin (tribromoethanol; Sigma-Aldrich), the skin and fatty tissue over iLN were removed. The mouse was placed in a prewarmed coverglass chamber slide (Nalgene; Nunc). The chamber slide was then placed into the temperature control chamber (The Cube and Box; Life Imaging Services) equipped on the microscope (SP5; Leica). The temperature of air was monitored and maintained at 37.0°C ± 0.5°C. iLN was intravitally imaged from the capsule over a range of depths (60–220 μm). Two-photon imaging was performed with an inverted five-channel confocal microscope (SP5) equipped with a 20× multi-immersion objective, 0.7 NA (immersion medium used 80% glycerol). Two-photon excitation was provided by a Mai Tai Ti:Sapphire laser (Spectra Physics) with a 10 W pump, tuned to 810 nm. Emitted fluorescence was collected using a four-channel nondescanned detector. Wavelength separation was through a dichroic mirror at 495 nm and then separated again through a dichroic mirror at 455 nm, followed by 405/20 nm emission filter for second harmonics and 480/40 nm emission filter for CMF_2HC, and a dichroic mirror at 565 nm, followed by 525/50 nm emission filter for CMFDA and 620/60 nm emission filter for Alexa Fluor 594 (Invitrogen). For four-dimensional analysis of cell migration, stacks of 4 or 10 sections (z step = 3 μm) were acquired every 15 or 30 s to provide an imaging volume of 9 or 27 μm in depth. To visualize TLR4-stimulated B cells in germinal centers, B6 recipient mice were injected subcutaneously with 100 μg HEL (Sigma-Aldrich) in CFA. 6–10 d later, 7–10 million LPS-activated or nonactivated splenic B cells were adoptively transferred intravenously into immunized mice and 10 μg FDC-M2 (ImmunoKontact) conjugated to Alexa Fluor 594 (Invitrogen) was injected subcutaneously. In some instances, HEL-transgenic B cells were transferred. Imaging was performed as indicated in this section. Sequences of image stacks were transformed into volume-rendered four-dimensional videos using Imaris software (v.6.0.1; Bitplane), and the spot analysis was used for semiautomated tracking of cell motility in three dimensions using the following parameters: autoregressive motion algorithm, estimated diameter 10 μm, background subtraction true, maximum distance 20 μm, and maximum gap size 3. The dataset was corrected for tissue drift by the Imaris software. Calculations of the cell velocity and displacement were performed using the Imaris software. All statistical analysis was performed with Prism (GraphPad Software, Inc.). Significance of statistics was calculated with unpaired *t* test for two nonparametric data.

TP-LSM images of cryostat section of spleens. Fluorescently stained wild-type B cells (blue; CMF_2HC) and 1 μg/ml LPS (overnight)-pulsed GFP–B cells (green) were adoptively transferred into the recipient mouse previously immunized with 100 μg of emulsified HEL-CFA for 7 d. 1 d before sacrifice, 10 μg of Alexa Fluor 594–conjugated anti–FDC-M2 antibody was injected subcutaneously in the region of the iLN. 4 d after cell transfer, the spleen was collected and then fixed with a periodate-lysine-paraformaldehyde fixative solution for 12 h and then dehydrated with 30% sucrose in phosphate buffer. OCT-embedded 100-μm cryostat section was mounted with Vectashield (Vector Laboratories) mounting medium. Imaging was performed as indicated in the previous section.

Homing assays. LPS-activated or nonactivated B cells from C57BL/6 were labeled with 1 μM CMFDA or 2.5 μM CMTMR for 15 min at 37°C and equal numbers of viable cells (7–20 million) were injected intravenously into recipient mice. After 2 h, spleen, iLNs, and pLNs were removed and gently dissociated into single cell suspensions. Peripheral blood was collected by retro-orbital eye bleeding. After removing red blood cells with Tris-NH_4Cl, the cells were resuspended in PBS containing 1% BSA at 4°C. Flow cytometric analysis was performed on a FACSCalibur or CANTO II and the data were analyzed using the FlowJo software. Forward and side scatter parameters were used to gate on live cells.

LN transit assay. The assay was performed as previously described (Han et al., 2005). LPS-activated or non–LPS-activated B cells from C57BL/6 were labeled with 2 μM CMFDA or 2.5 μM CMTMR for 15 min at 37°C and 7–20 million viable cells of each population were injected intravenously to recipient mice. 2 h later, the mice were injected intravenously with either PBS or anti–L-selectin antibody (100 μg/mouse). After 12 and 24 h, iLNs and pLNs were removed and gently dissociated into single cell suspensions. Peripheral blood was collected by retro-orbital eye bleeding. After removing red blood cells with Tris-NH_4Cl, the cells were resuspended in PBS containing 1% BSA at 4°C. Flow cytometric analysis was performed on a FACSCalibur or CANTO II and the data were analyzed using FlowJo software. Forward and side scatter parameters were used to gate on live cells.

Measurement of HEL-specific antibody responses. Two groups of five mice (6 wk old, C57BL/6 CD45.2) were injected subcutaneously on both sides of the iLN on day 0 with 100 μg HEL in CFA (HEL + CFA, 1:1 vol/vol in stable emulsion) in a 100-μl final volume. 15 million cells of LPS-activated or non–LPS-activated B cells from C57BL/6 CD45.1 mice were injected intravenously into recipient mice on day 7. Mice were boosted on day 28 with 100 μg Hel antigen. They were bled on day −1, day 28, and day 38 from mouse tail. Serum was obtained after clotting at room temperature and centrifugation for 5 min at 10,000 *g*. HEL-specific antibody responses were assayed by ELISA, as described in Moratz et al. (2004). In brief, 96-well ELISA plates (Costar) were coated with 10 μg/ml Hel antigen (Sigma-Aldrich) overnight at 4°C, washed, and blocked with 1% bovine serum albumin fraction V (Sigma-Aldrich). Serial dilutions of serum were then added to the plates and incubated 4 h at 4°C. After washing, alkaline phosphatase–conjugated goat anti–mouse Ig isotype antibodies (SouthernBiotech) were added for 2 h at room temperature. Absorbance was then measured at 405 nm in a Flexstation 3 (MDS Analytical Technologies). The results were expressed as absorbance units at OD_{405} ± SD.

Immunohistochemistry. A similar immunization and transfer protocol was used as for measuring the HEL-specific antibody response. Freshly isolated day-38 spleens were snap frozen in Tissue-Tek OCT compound (Sakura). 7-μm frozen OCT splenic sections were acetone fixed for 2 min and dried at room temperature. Slides were rehydrated in Tris-buffered saline and stained in a humidified chamber in Tris-buffered saline/0.1% BSA/1% mouse serum overnight at 4°C or for 1 h at room temperature. Primary antibodies included mouse anti–mouse CD45.1 (A20, biotinylated; BD) and Armenian hamster anti–mouse CD3e (145-2C11, purified; BD). Also used were rat anti–mouse IgD (11-26c.2a, purified; BD), rat anti–mouse CD35 (8C12, biotinylated; BD), and rat anti–mouse MAdCAM-1 (MECA-367, purified; BD). Biotinylated antibodies were detected with streptavidin-alkaline phosphatase (Jackson ImmunoResearch Laboratories) and purified mAbs with AP-conjugated goat anti–Armenian hamster IgG (H+L; Jackson ImmunoResearch Laboratories) or HRP-conjugated donkey anti–rat IgG (H+L; Jackson ImmunoResearch Laboratories). HRP was reacted with DAB (Peroxidase Substrate kit; Vector Laboratories) and alkaline phosphatase was reacted with Fast blue/Napthol (AS-MX; Sigma-Aldrich). Levamisole (Sigma-Aldrich) was used to block endogenous alkaline phosphatase activity. Slides were mounted in Crystal Mount (Electron Microscopy Sciences). Images were acquired with a microscope (BX-50; Olympus) equipped with a ProgRes digital microscope camera (Jenoptik) and assembled using Photoshop CS (Adobe).

Analysis of transferred GFP-positive B cells. Two groups of four mice (6 wk old, C57BL/6) were injected subcutaneously near the left iLN on day

0 with 100 μg HEL in CFA. 25 million LPS-activated or non–LPS-activated GFP B cells from C57BL/6-Tg(UBC-GFP)30Scha/J were injected intravenously into the recipient mice on day 7. Mice were boosted on day 21 with 100 μg HEL in PBS. At day 42, spleen, iLNs and femurs were removed and gently dissociated into single cell suspensions. After removing red blood cells with Tris-NH_4Cl, the cells were resuspended in PBS containing 1% BSA at 4°C. Flow cytometric analysis was performed on a FACSCanto II and the data were analyzed using FlowJo software. Forward and side scatter parameters were used to gate on live cells.

Statistics. In vivo results represent samples from three to six mice per experiment. In vitro results represent mean values of sextuplet samples. All experiments were performed at least three times. SD and p-values were calculated with the Student's *t* test using Excel (Microsoft) or Prism software.

Online supplemental material. Fig. S1 compares receptor expression of freshly isolated splenic B cells versus B cells stimulated with LPS overnight and shows the enhanced chemotactic responses of the LPS-stimulated B cells. Fig. S2 shows the distances from the follicle edge of LPS and nonactivated B cells. Fig. S3 shows by immunohistochemistry the location of the LPS-stimulated B cells in the dark zone of a germinal center. Fig. S4 shows that the transfer of TLR4 ligand–exposed B cells enhanced a HEL-specific antibody response. Fig. S5 shows the presence of LPS-stimulated and transferred B cells in germinal center present in the spleen of HEL-boosted mice. Video 1 shows the results of intravital microscopy of LPS and nonactivated B cells in the iLN of an anesthetized mouse. Video 2 shows the tracking of TLR4-stimulated B cells 48 h after transfer in the iLN. Video 3 shows the results of intravital microscopy of TLR4-stimulated B cells located in the light zone of an iLN germinal center. Video 4 shows TLR4-stimulated B cells in the dark zone of the germinal center. Video 5 compares TLR4-activated B cells to antigen-specific B cells after transfer to a previously immunized recipient mouse visualized by intravital microscopy. Video 6 shows TLR4-stimulated B cells dividing in a LN germinal center. Online supplemental material is available at http://www.jem.org/cgi/content/full/jem.20091982/DC1.

The authors would like to thank Mary Rust for excellent editorial assistance; Dr. Owen Schwartz, Meggan Czapiga, and Dr. Juraj Kabat of the Research Technology Branch for their support with the TP-LSM; and Dr. Anthony Fauci for his continued support.

This research was supported by the Intramural Research Program of the National Institute of Allergy and Infectious Diseases, National Institutes of Health.

The authors have no conflicting financial interests.

Submitted: 11 September 2009
Accepted: 21 October 2009

REFERENCES

Allen, C.D., K.M. Ansel, C. Low, R. Lesley, H. Tamamura, N. Fujii, and J.G. Cyster. 2004. Germinal center dark and light zone organization is mediated by CXCR4 and CXCR5. *Nat. Immunol.* 5:943–952. doi:10.1038/ni1100

Allen, C.D., T. Okada, H.L. Tang, and J.G. Cyster. 2007. Imaging of germinal center selection events during affinity maturation. *Science*. 315:528–531. doi:10.1126/science.1136736

Aloisi, F., and R. Pujol-Borrell. 2006. Lymphoid neogenesis in chronic inflammatory diseases. *Nat. Rev. Immunol.* 6:205–217. doi:10.1038/nri1786

Anderson, S.M., M.M. Tomayko, A. Ahuja, A.M. Haberman, and M.J. Shlomchik. 2007. New markers for murine memory B cells that define mutated and unmutated subsets. *J. Exp. Med.* 204:2103–2114. doi:10.1084/jem.20062571

Bajénoff, M., J.G. Egen, L.Y. Koo, J.P. Laugier, F. Brau, N. Glaichenhaus, and R.N. Germain. 2006. Stromal cell networks regulate lymphocyte entry, migration, and territoriality in lymph nodes. *Immunity*. 25:989–1001. doi:10.1016/j.immuni.2006.10.011

Benson, M.J., L.D. Erickson, M.W. Gleeson, and R.J. Noelle. 2007. Affinity of antigen encounter and other early B-cell signals determine B-cell fate. *Curr. Opin. Immunol.* 19:275–280. doi:10.1016/j.coi.2007.04.009

Bernasconi, N.L., N. Onai, and A. Lanzavecchia. 2003. A role for Toll-like receptors in acquired immunity: up-regulation of TLR9 by BCR triggering in naive B cells and constitutive expression in memory B cells. *Blood*. 101:4500–4504. doi:10.1182/blood-2002-11-3569

Beutler, B., and E.T. Rietschel. 2003. Innate immune sensing and its roots: the story of endotoxin. *Nat. Rev. Immunol.* 3:169–176. doi:10.1038/nri1004

Cappione, A. III, J.H. Anolik, A. Pugh-Bernard, J. Barnard, P. Dutcher, G. Silverman, and I. Sanz. 2005. Germinal center exclusion of autoreactive B cells is defective in human systemic lupus erythematosus. *J. Clin. Invest.* 115:3205–3216. doi:10.1172/JCI24179

Cyster, J.G. 2005. Chemokines, sphingosine-1-phosphate, and cell migration in secondary lymphoid organs. *Annu. Rev. Immunol.* 23:127–159. doi:10.1146/annurev.immunol.23.021704.115628

Ding, C., L. Wang, H. Al-Ghawi, J. Marroquin, M. Mamula, and J. Yan. 2006. Toll-like receptor engagement stimulates anti-snRNP autoreactive B cells for activation. *Eur. J. Immunol.* 36:2013–2024. doi:10.1002/eji.200635850

Freitas, A.A., and M. de Sousa. 1976. Control mechanism of lymphocyte traffic. Altered distribution of 51Cr-labeled mouse lymph node cells pretreated in vitro with lipopolysaccharide. *Eur. J. Immunol.* 6:269–273. doi:10.1002/eji.1830060407

Gargano, L.M., J.M. Moser, and S.H. Speck. 2008. Role for MyD88 signaling in murine gammaherpesvirus 68 latency. *J. Virol.* 82:3853–3863. doi:10.1128/JVI.02577-07

Gavin, A.L., K. Hoebe, B. Duong, T. Ota, C. Martin, B. Beutler, and D. Nemazee. 2006. Adjuvant-enhanced antibody responses in the absence of toll-like receptor signaling. *Science*. 314:1936–1938. doi:10.1126/science.1135299

Goodlad, J.R., and J.C. Macartney. 1995. Germinal-center cell proliferation in response to T-independent antigens: a stathmokinetic, morphometric and immunohistochemical study in vivo. *Eur. J. Immunol.* 25:1918–1926. doi:10.1002/eji.1830250719

Groom, J.R., C.A. Fletcher, S.N. Walters, S.T. Grey, S.V. Watt, M.J. Sweet, M.J. Smyth, C.R. Mackay, and F. Mackay. 2007. BAFF and MyD88 signals promote a lupuslike disease independent of T cells. *J. Exp. Med.* 204:1959–1971. doi:10.1084/jem.20062567

Han, S.B., C. Moratz, N.N. Huang, B. Kelsall, H. Cho, C.S. Shi, O. Schwartz, and J.H. Kehrl. 2005. Rgs1 and Gnai2 regulate the entrance of B lymphocytes into lymph nodes and B cell motility within lymph node follicles. *Immunity*. 22:343–354. doi:10.1016/j.immuni.2005.01.017

Hanten, J.A., J.P. Vasilakos, C.L. Riter, L. Neys, K.E. Lipson, S.S. Alkan, and W. Birmachu. 2008. Comparison of human B cell activation by TLR7 and TLR9 agonists. *BMC Immunol.* 9:39–54. doi:10.1186/1471-2172-9-39

Hauser, A.E., T. Junt, T.R. Mempel, M.W. Sneddon, S.H. Kleinstein, S.E. Henrickson, U.H. von Andrian, M.J. Shlomchik, and A.M. Haberman. 2007. Definition of germinal-center B cell migration in vivo reveals predominant intrazonal circulation patterns. *Immunity*. 26:655–667. doi:10.1016/j.immuni.2007.04.008

Hawkins, E.D., M. Hommel, M.L. Turner, F.L. Battye, J.F. Markham, and P.D. Hodgkin. 2007. Measuring lymphocyte proliferation, survival and differentiation using CFSE time-series data. *Nat. Protoc.* 2:2057–2067. doi:10.1038/nprot.2007.297

Herlands, R.A., S.R. Christensen, R.A. Sweet, U. Hershberg, and M.J. Shlomchik. 2008. T cell-independent and toll-like receptor-dependent antigen-driven activation of autoreactive B cells. *Immunity*. 29:249–260. doi:10.1016/j.immuni.2008.06.009

Horie, K., and H. Hoshi. 1989. Induction of lymph follicle formation with several mitogens and adjuvants in the mouse popliteal lymph node. *Histol. Histopathol.* 4:17–25.

Hsu, H.C., P. Yang, J. Wang, Q. Wu, R. Myers, J. Chen, J. Yi, T. Guentert, A. Tousson, A.L. Stanus, et al. 2008. Interleukin 17-producing T helper cells and interleukin 17 orchestrate autoreactive germinal center development in autoimmune BXD2 mice. *Nat. Immunol.* 9:166–175. doi:10.1038/ni1552

Huber, C., C. Thielen, H. Seeger, P. Schwarz, F. Montrasio, M.R. Wilson, E. Heinen, Y.X. Fu, G. Miele, and A. Aguzzi. 2005. Lymphotoxin-beta receptor-dependent genes in lymph node and follicular dendritic cell transcriptomes. *J. Immunol.* 174:5526–5536.

Hwang, I.Y., C. Park, and J.H. Kehrl. 2007. Impaired trafficking of Gnai2+/- and Gnai2-/- T lymphocytes: implications for T cell movement within lymph nodes. *J. Immunol.* 179:439–448.

Jacob, J., G. Kelsoe, K. Rajewsky, and U. Weiss. 1991. Intraclonal generation of antibody mutants in germinal centres. *Nature.* 354:389–392. doi:10.1038/354389a0

Klein, U., and R. Dalla-Favera. 2008. Germinal centres: role in B-cell physiology and malignancy. *Nat. Rev. Immunol.* 8:22–33. doi:10.1038/nri2217

Krieg, A.M., and J. Vollmer. 2007. Toll-like receptors 7, 8, and 9: linking innate immunity to autoimmunity. *Immunol. Rev.* 220:251–269. doi:10.1111/j.1600-065X.2007.00572.x

Lanzavecchia, A., and F. Sallusto. 2007. Toll-like receptors and innate immunity in B-cell activation and antibody responses. *Curr. Opin. Immunol.* 19:268–274. doi:10.1016/j.coi.2007.04.002

Leadbetter, E.A., I.R. Rifkin, A.M. Hohlbaum, B.C. Beaudette, M.J. Shlomchik, and A. Marshak-Rothstein. 2002. Chromatin-IgG complexes activate B cells by dual engagement of IgM and Toll-like receptors. *Nature.* 416:603–607. doi:10.1038/416603a

Liu, B., Y. Yang, J. Dai, R. Medzhitov, M.A. Freudenberg, P.L. Zhang, and Z. Li. 2006. TLR4 up-regulation at protein or gene level is pathogenic for lupus-like autoimmune disease. *J. Immunol.* 177:6880–6888.

Liu, Y.J., S. Oldfield, and I.C. MacLennan. 1988. Memory B cells in T cell-dependent antibody responses colonize the splenic marginal zones. *Eur. J. Immunol.* 18:355–362. doi:10.1002/eji.1830180306

Liu, Y.J., D.E. Joshua, G.T. Williams, C.A. Smith, J. Gordon, and I.C. MacLennan. 1989. Mechanism of antigen-driven selection in germinal centres. *Nature.* 342:929–931. doi:10.1038/342929a0

Luzina, I.G., S.P. Atamas, C.E. Storrer, L.C. daSilva, G. Kelsoe, J.C. Papadimitriou, and B.S. Handwerger. 2001. Spontaneous formation of germinal centers in autoimmune mice. *J. Leukoc. Biol.* 70:578–584.

MacLennan, I.C. 1994. Germinal centers. *Annu. Rev. Immunol.* 12:117–139. doi:10.1146/annurev.iy.12.040194.001001

Meyer-Bahlburg, A., S. Khim, and D.J. Rawlings. 2007. B cell–intrinsic TLR signals amplify but are not required for humoral immunity. *J. Exp. Med.* 204:3095–3101. doi:10.1084/jem.20071250

Miller, M.J., S.H. Wei, I. Parker, and M.D. Cahalan. 2002. Two-photon imaging of lymphocyte motility and antigen response in intact lymph node. *Science.* 296:1869–1873. doi:10.1126/science.1070051

Moratz, C., J.R. Hayman, H. Gu, and J.H. Kehrl. 2004. Abnormal B-cell responses to chemokines, disturbed plasma cell localization, and distorted immune tissue architecture in Rgs1-/- mice. *Mol. Cell. Biol.* 24:5767–5775. doi:10.1128/MCB.24.13.5767-5775.2004

Muramatsu, M., K. Kinoshita, S. Fagarasan, S. Yamada, Y. Shinkai, and T. Honjo. 2000. Class switch recombination and hypermutation require activation-induced cytidine deaminase (AID), a potential RNA editing enzyme. *Cell.* 102:553–563. doi:10.1016/S0092-8674(00)00078-7

Okada, T., M.J. Miller, I. Parker, M.F. Krummel, M. Neighbors, S.B. Hartley, A. O'Garra, M.D. Cahalan, and J.G. Cyster. 2005. Antigen-engaged B cells undergo chemotaxis toward the T zone and form motile conjugates with helper T cells. *PLoS Biol.* 3:e150. doi:10.1371/journal.pbio.0030150

Pasare, C., and R. Medzhitov. 2005. Control of B-cell responses by Toll-like receptors. *Nature.* 438:364–368. doi:10.1038/nature04267

Paus, D., T.G. Phan, T.D. Chan, S. Gardam, A. Basten, and R. Brink. 2006. Antigen recognition strength regulates the choice between extrafollicular plasma cell and germinal center B cell differentiation. *J. Exp. Med.* 203:1081–1091. doi:10.1084/jem.20060087

Peng, S.L. 2005. Signaling in B cells via Toll-like receptors. *Curr. Opin. Immunol.* 17:230–236. doi:10.1016/j.coi.2005.03.003

Quah, B.J., H.S. Warren, and C.R. Parish. 2007. Monitoring lymphocyte proliferation in vitro and in vivo with the intracellular fluorescent dye carboxyfluorescein diacetate succinimidyl ester. *Nat. Protoc.* 2:2049–2056. doi:10.1038/nprot.2007.296

Reif, K., E.H. Ekland, L. Ohl, H. Nakano, M. Lipp, R. Förster, and J.G. Cyster. 2002. Balanced responsiveness to chemoattractants from adjacent zones determines B-cell position. *Nature.* 416:94–99. doi:10.1038/416094a

Ruprecht, C.R., and A. Lanzavecchia. 2006. Toll-like receptor stimulation as a third signal required for activation of human naive B cells. *Eur. J. Immunol.* 36:810–816. doi:10.1002/eji.200535744

Schaniel, C., E. Pardali, F. Sallusto, M. Speletas, C. Ruedl, T. Shimizu, T. Seidl, J. Andersson, F. Melchers, A.G. Rolink, and P. Sideras. 1998. Activated murine B lymphocytes and dendritic cells produce a novel CC chemokine which acts selectively on activated T cells. *J. Exp. Med.* 188:451–463. doi:10.1084/jem.188.3.451

Schaniel, C., F. Sallusto, C. Ruedl, P. Sideras, F. Melchers, and A.G. Rolink. 1999. Three chemokines with potential functions in T lymphocyte-independent and -dependent B lymphocyte stimulation. *Eur. J. Immunol.* 29:2934–2947. doi:10.1002/(SICI)1521-4141(199909)29:09<2934::AID-IMMU2934>3.0.CO;2-Q

Schwickert, T.A., R.L. Lindquist, G. Shakhar, G. Livshits, D. Skokos, M.H. Kosco-Vilbois, M.L. Dustin, and M.C. Nussenzweig. 2007. In vivo imaging of germinal centres reveals a dynamic open structure. *Nature.* 446:83–87. doi:10.1038/nature05573

Shi, G.X., K. Harrison, S.B. Han, C. Moratz, and J.H. Kehrl. 2004. Toll-like receptor signaling alters the expression of regulator of G protein signaling proteins in dendritic cells: implications for G protein-coupled receptor signaling. *J. Immunol.* 172:5175–5184.

Souvannavong, V., C. Lemaire, and R. Chaby. 2004. Lipopolysaccharide protects primary B lymphocytes from apoptosis by preventing mitochondrial dysfunction and bax translocation to mitochondria. *Infect. Immun.* 72:3260–3266. doi:10.1128/IAI.72.6.3260-3266.2004

Tarlinton, D.M. 2008. Evolution in miniature: selection, survival and distribution of antigen reactive cells in the germinal centre. *Immunol. Cell Biol.* 86:133–138. doi:10.1038/sj.icb.7100148

Taylor, P.R., M.C. Pickering, M.H. Kosco-Vilbois, M.J. Walport, M. Botto, S. Gordon, and L. Martinez-Pomares. 2002. The follicular dendritic cell restricted epitope, FDC-M2, is complement C4; localization of immune complexes in mouse tissues. *Eur. J. Immunol.* 32:1888–1896.

William, J., C. Euler, S. Christensen, and M.J. Shlomchik. 2002. Evolution of autoantibody responses via somatic hypermutation outside of germinal centers. *Science.* 297:2066–2070. doi:10.1126/science.1073924

William, J., C. Euler, N. Primarolo, and M.J. Shlomchik. 2006. B cell tolerance checkpoints that restrict pathways of antigen-driven differentiation. *J. Immunol.* 176:2142–2151.